CHEMISTRY OF DIOGENITES AND EVOLUTION OF THEIR PARENT ASTEROID.

D. W. Mittlefehldt[1] A. W. Beck[2], C.-T. A. Lee[3] and H. Y. McSween Jr.[2], [1]Astromaterials Research Office, NASA/Johnson Space Center, Houston, TX, USA (david.w.mittlefehldt@nasa.gov), [2]Dept. of Earth and Planetary Sciences, University of Tennessee, Knoxville, TN, USA, [3]Dept. of Earth Science, Rice University, Houston, TX, USA.

Introduction: Diogenites are orthopyroxenite meteorites [1]. Most are breccias, but remnant textures indicate they were originally coarse-grained rocks, with grain sizes of order of cm. Their petrography, and major and trace element chemistry support an origin as crustal cumulates from a differentiated asteroid. Diogenites are genetically related to the basaltic and cumulate-gabbro eucrites, and the polymict breccias known as howardites, collectively, the HED suite. Spectroscopic observations, orbit data and dynamical arguments strongly support the hypothesis that asteroid 4 Vesta is the parent object for HED meteorites [2]. Here we discuss our new trace element data for a suite of diogenites and integrate these into the body of literature data. We use the combined data set to discuss the petrologic evolution of diogenites and 4 Vesta.

Samples and Methods: The samples studied here are mostly meteorites recovered since 1995, plus some older samples that had not been extensively studied. Interior samples were studied. In some cases, orthopyroxene clasts were separated for analysis; in others bulk samples were used. Two types of analyses were done. Our earlier analyses were done by INAA at JSC using the procedures detailed in [3]. Some of these data have been discussed previously [4]. The most recent analyses were done by ICP-MS at Rice University using the procedures described in [5]. All of these samples are termed "new" diogenites here, and we have averaged our data with literature data. Literature averages for diogenites not analyzed here, termed "old," are also used in the discussion.

Diogenites are coarse-grained rocks, and sample representativeness is a worry. Using averaged data only partially mitigates this worry. Nevertheless, comparison of data from extensively studied diogenites suggests that the data distribution is not an artifact of sampling.

Results: The new diogenites extend the ranges in major and incompatible lithophile element compositions. MET 00425 is the most magnesian diogenite with an orthopyroxene mg # of 83.8, compared to ~79-80 for the next most magnesian, and has the lowest Sc content (Fig. 1). LEW 88008 is among the most ferroan (mg# 68.8, like that of Yamato Type B diogenites) and has the highest Sc content, excluding anomalous diogenite Dhofar 700 [6] (Fig. 1). Three new diogenites are notable for having low rare-earth-element contents - MET 00422, MET 00424 and MET 00436 (Figs. 2, 3).

Discussion: Diogenites are thought to have formed via fractional crystallization [1]. Petrologic and trace element studies have led to the hypotheses that multiple parent magmas are required, and that post-crystallization equilibration decoupled the pyroxene mg# from the minor and trace element distributions [3, 7, 8]. One model for petrogenesis of the HED parent asteroid is that a totally molten asteroid underwent fractional crystallization to produce the diogenite and eucrite crustal suites, plus a dunitic mantle and a metallic core [9]. Can the inference of multiple parent magmas from diogenite data be reconciled with modeling of HED petrogenesis that implies a single global magma?

Modeling was done using the melt evolution results of [9] and partition coefficients calculated after [10]. The Sc partition coefficients varied with melt composition (see [10]) and the modeling was done as a series of discrete steps. (Models shown are based on the olivine-rich "HED-CI" model of [9], with chondritic ratios of Sc/Al, Sm/Al and Yb/Al. Other models [9] were also tested.) The orthopyroxene cumulate track lies to the high mg#, high Sc side of the data field in Fig. 1, and does not provide a good match to diogenites. Allowing for a trapped melt component that equilibrated with the cumulate can obviate some of the discrepancy, but not all of it. Most diogenites have lower Sc contents for a given pyroxene mg# than model cumulate-trapped melt mixes would predict (Fig. 1). Also, the more ferroan diogenites would require 60-70% of a trapped melt component to bring the bulk mg# to measured values. The model melt has about 24 vol% normative plagioclase. The mixing model for LEW 88008 (Fig. 1) would then predict it should contain ~16 vol% plagioclase, compared to a measured mode of only 2% [11].

The same model is somewhat better at matching the distribution of Yb-Sc and Sm-Sc data for most diogenites (Figs. 2, 3). However, note that most diogenites require >5% trapped melt to explain the Yb-Sc data, while about half require <5% trapped melt for Sm-Sc. Thus, internal consistency is lacking. The initial melt used in the calculation assumed chondritic ratios for the elements. Relaxing this assumption by allowing the parent melt to have been LREE-depleted does not alleviate the problem, nor does adjusting the partition coefficients within reasonable limits. Thus, this particular crystallization model ("HED-CI" of [9]) cannot explain the lithophile trace element variations within the diogenite suite.

The "HED-CI" model does not yield cumulate orthopyroxene with Sc contents as low as observed for magnesian diogenites (Fig. 1) The pyroxene-rich "HED-EH" model [9] can replicate the lower Sc contents, but has the same problems explaining the Yb-Sc and Sm-Sc distributions. We have been unable to find a fractional crystallization model that recovers the mg#, Sc and REE characteristics of the diogenite suite.

Some diogenites are just inexplicable by any simple model. The Yb content of MET 00424 is roughly a factor of 6 below the hypothetical cumulate (Fig. 2). The estimated Yb content for magma in equilibrium with MET 00424 is ~0.1 times CI chondrites. This is implausible for any magma generated via total asteroid melting or equilibrium partial melting. Such low REE contents may be realized in melts formed by fractional fusion [3, 12], or in cumulates that were subsequently remelted [6, 13]. Either scenario implies a more complex petrogenesis for 4 Vesta than typically envisioned in global melting models.

Acknowledgement: We thank A. Ruzicka for making detailed output from his HED parent asteroid modeling available for our use.

References: [1] Mittlefehldt D.W. *et al.* (1998) *Planetary Materials*, RiM **36,** Ch. 4. [2] Binzel R.P. & Xu S. (1993) *Science* **260,** 186. [3] Mittlefehldt D.W. (1994) *Geochim. Cosmochim. Acta* **58,** 1537. [4] Mittlefehldt D.W. (2002) *Meteoritics Planet. Sci.* **37,** A100. [5] Lee C.-T.A. *et al.* (2006) *Contrib. Mineral. Petrol.* **151,** 122. [6] Barrat J.-A. *et al.* (2008) *Meteoritics Planet. Sci.*, in press. [7] Fowler G.W. *et al.* (1995) *Geochim. Cosmochim. Acta* **59,** 3071. [8] Shearer C.K. *et al.* (1997) *Meteoritics Planet. Sci.* **32,** 877. [9] Ruzicka A. *et al.* (1997) *Meteoritics Planet. Sci.* **32,** 825. [10] Jones J. H. (1995) *Rock Physics and Phase Relations, A Handbook of Physical Constants,* AGU, 73. [11] Bowman L.E. *et al.* (1997) *Meteoritics Planet. Sci.* **32,** 869. [12] Stolper E. (1977) *Geochim. Cosmochim. Acta* **41,** 587. [13] Fukuoka et al. (1977) *Proc. 8th Lunar Sci. Conf.*, 187.

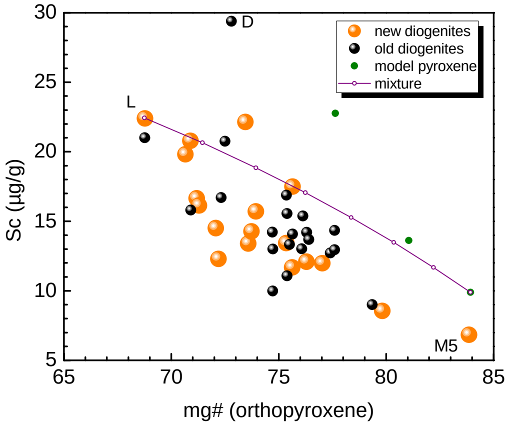

Figure 1. Bulk rock Sc *vs.* orthopyroxene mg# for diogenites and model cumulate pyroxenes. "New" and "old" are defined in the text. Mixture shows the effects of adding trapped melt in 10% increments. Labeled meteorites: D – Dhofar 700; L – LEW 88008; M5 - MET 00425.

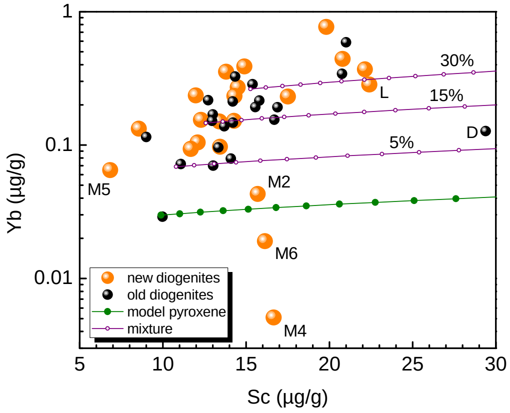

Figure 2. Yb *vs.* Sc for diogenites compared to a model crystallization track. Mixture tracks show the effects of adding 5%, 15% and 30% trapped melt. Additional labeled meteorites: M2 – MET 00422; M4 – MET 00424; M6 – MET 00436.

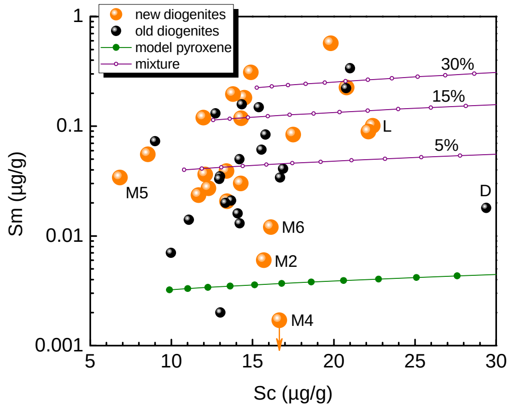

Figure 3. Sm *vs.* Sc for diogenites compared to a model crystallization track. Mixture tracks show the effects of adding 5%, 15% and 30% trapped melt. The plotted Sm content of MET 00424 is a 2σ upper limit.